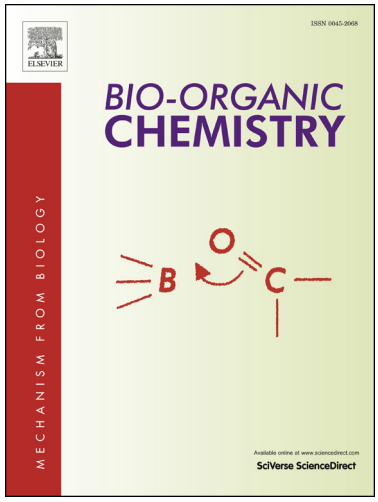

One-Pot Synthesis of Tetrazole-1,2,5,6-Tetrahydronicotinonitriles and Cholinesterase Inhibition: Probing the Plausible Reaction Mechanism *via* Computational Studies

Abdul Hameed, Syeda Tazeen Zehra, Saba Abbas, Riffat Un Nisa, Tariq Mahmood, Khurshid Ayub, Mariya al-Rashida, Jürgen Bajorath, Khalid Mohammed Khan, Jamshed Iqbal

PII: S0045-2068(16)30004-9
DOI: http://dx.doi.org/10.1016/j.bioorg.2016.01.004
Reference: YBIOO 1872

To appear in: *Bioorganic Chemistry*

Received Date: 26 December 2015
Revised Date: 18 January 2016
Accepted Date: 18 January 2016

Please cite this article as: A. Hameed, S.T. Zehra, S. Abbas, R.U. Nisa, T. Mahmood, K. Ayub, M. al-Rashida, J. Bajorath, K.M. Khan, J. Iqbal, One-Pot Synthesis of Tetrazole-1,2,5,6-Tetrahydronicotinonitriles and Cholinesterase Inhibition: Probing the Plausible Reaction Mechanism *via* Computational Studies, *Bioorganic Chemistry* (2016), doi: http://dx.doi.org/10.1016/j.bioorg.2016.01.004

One-Pot Synthesis of Tetrazole-1,2,5,6-Tetrahydronicotinonitriles and Cholinesterase Inhibition: Probing the Plausible Reaction Mechanism *via* Computational Studies

Abdul Hameed[*a], Syeda Tazeen Zehra[a], Saba Abbas[b], Riffat Un Nisa[c], Tariq Mahmood[c], Khurshid Ayub[c], Mariya al-Rashida[d], Jürgen Bajorath[e], Khalid Mohammed Khan[a], and Jamshed Iqbal[*b]

[a] H. E. J. Research Institute of Chemistry, International Center for Chemical and Biological Sciences, University of Karachi, Karachi-75270, Pakistan.

[b]Center for Advanced Drug Research, COMSATS Institute of Information Technology, Abbottabad 22060, Pakistan.

[c] Department of Chemistry, COMSATS, Institute of Information Technology, Abbottabad 22060, Pakistan.

[d]Department of Chemistry, Forman Christian College (A Chartered University), Ferozepur Road-54600, Lahore, Pakistan

[e]Department of Life Science Informatics, B-IT, LIMES Program Unit Chemical Biology and Medicinal Chemistry, Rheinische Friedrich-Wilhelms-Universität, Dahlmann str. 2, D-53113 Bonn, Germany

Abstract

In the present study, one-pot synthesis of 1*H*-tetrazole linked 1,2,5,6-tetrahydronicotinonitriles under solvent-free conditions have been carried out in the presence of tetra-*n*-butyl ammonium fluoride trihydrated (TBAF) as catalyst and solvent. Computational studies have been conducted to elaborate two plausible mechanistic pathways of this one-pot reaction. Moreover, the synthesized compounds were screened for cholinesterases (acetylcholinesterase and butyrylcholinesterase) inhibition which are consider to be major malefactors of Alzheimer's disease (AD) to find lead compounds for further research in AD therapy.

Keywords: Ionic liquids, Click chemistry, Tetrazole, 1,2,5,6-Tetrahydronicotinonitrile, Density Functional Theory (DFT), Acetylcholinesterase (AChE), Butyrylcholinesterase (BChE)

[*]Corresponding Authors: A.H. Tel.: 0092-21-99261701-2; Fax: 0092-21-3481901; abdul.hameed@iccs.edu
J.I., Tel.: +92-992-383591-96; fax: +92-992-383441; e-mail: drjamshed@ciit.net.pk

1. Introduction

Solvent-free chemistry holds a unique place in organic synthesis to reduce environmental hazards. The reaction avoids the use of toxic and volatile conventional organic solvents. For solvent-free reactions ionic liquids provide excellent media for organic syntheses. Ionic liquids serve as catalysts in many organic reactions [1]. Tetra-*n*-butylammonium fluoride (TBAF) is a type of an ionic liquid that has been diversely used in organic syntheses. A range of different solvent-free reactions have also been performed in the presence of TBAF as catalyst. Fluoride (F^-) counter anion present in TBAF serves as mild base to promote different chemical reactions [2-4]. In our solvent-free chemistry, a one-pot reaction between acetophenone, malononitrile and trimethylsilyl azide ($TMSN_3$) was explored in the presence of neat TBAF to afford tetrazole linked 1,2,5,6-tetrahydronicotinonitriles **2(a-h)**. The reaction involved 1) fluoride (F^-) mediated Knoevenagel condensation 2) followed by multisteps ring closure to afford corresponding 1,2,5,6-tetrahydronicotinonitriles **(5)**. Consequently 3) the click reaction furnished tetrazole linked 1,2,5,6-tetrahydronicotinonitriles (**2)** (Scheme 1) [5]. Plausible mechanism of such interesting one-pot reaction upto intermediate **(5)** has been suggested by two different logical pathways **(I)** and **(II)** (Scheme 2) [5, 6]. The intermediate 1,2,5,6-tetrahydronicotinonitrile **(5)** also served as excellent precursor for the synthesis of [1,6]-naphthyridine ring system [5] found in many biological important molecules [7, 8].

Computational study using density field theory (DFT) calculations was carried out to elaborate the most feasible pathway of this one-pot reaction. The scope of reaction was explored with different phenyl substituted acetophenones. A series of tetrazole linked 1,2,5,6-tetrahydronicotinonitriles **2(a-h)** was synthesized under solvent-free conditions in moderate to excellent yield. The structures of compounds **2(a-h)** were confirmed using different spectroscopic techniques.

Medicinal chemistry has witnessed an expansion in the use of biologically active nicotine based molecules. Recently, Carreiras *et. al.* [9] synthesized nicotine containing pyridonepezils **(1)** and evaluated their inhibition activity against acetylcholinesterase (AChE) and butyrylcholinesterase (BChE). Based on close structural similarities of our synthetic tetrazole-1,2,5,6-tetrahydronicotinonitrile **(2)** with pyridonepezils **(1)** (Figure 1), we assessed them for their cholinesterases (AChE and BChE) inhibitory activities. According to so-called cholinergic hypothesis, [10, 11] cholinesterases are considered to be major responsible enzymes for the

pathogenesis of Alzheimer's disease (AD) complications. AD is a progressive neurodegenerative disorder that leads to gradual memory loss, decline in language skills and other effects on cognitive functions. A report from Alzheimer's disease international describes it as the most common type of dementia which now affects around 36 million people worldwide with 6% of the population being over the age of 65 [12-14]. The major factors contributing to Alzheimer's disease include 1) deposition of β-amyloid [15], 2) oxidative stress [16], 3) aggregation of tau protein [17], and 4) low level of acetylcholine due to severe loss of cholinergic cells in the brain.[10] Thus, the strategy to inhibit the activities of these enzymes is thought to provide opportunities for treatment of AD and its symptoms. It is now well-known that the AChE level is low in the presence of AD, while BChE shows an increased level. This suggests that BChE might be the more attractive target for selective AD therapy.

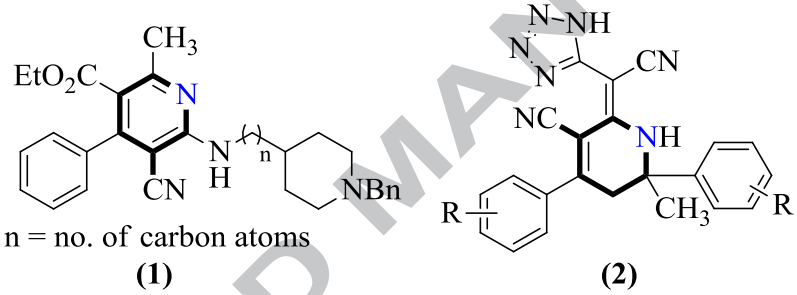

Figure-1: Structures of pyridonepezil **(1)** and tetrazole linked1,2,5,6-tetrahydronicotinonitrile **(2)**

2. Results and discussion

2.1 Chemistry

One-pot solvent-free synthesis of tetrazole linked 1,2,5,6-tetrahydronicotinonitrile derivatives **2(a-h**) was carried out using neat TBAF trihydrated as catalyst Scheme 1. Reaction between corresponding acetophenones (1 equiv.) and malononitrile (1.5 equiv.) first underwent Knoevenagel condensation to an *in situ* arylidene intermediate which *via* multisteps ring closure afforded 1,2,5,6-tetrahydronicotinonitrile **(5)**. Consequently, addition of azide furnished the tetrazole-linked 1,2,5,6-tetrahydronicotinonitrile **2(a-h)** in moderate to excellent yield. Two plausible mechanisms of this one-pot reaction have been shown in Scheme-2. The structures of final compounds **2(a-h)** have been elucidated with spectroscopic techniques including ^{1}H, C^{13} NMR spectroscopy *etc*. X-ray crystal structure of intermediate 2-dicyanomethylene-6-methyl-4,6-diphenyl-1,2,5,6-tetrahydronicotinonitrile **(5a)** has been reported in our previous publication

[18]. Tetrazole linked 1,2,5,6-tetrahydronicotinonitriles **2(a-h)** were further assessed for biological potential against cholinesterase, acetylcholinesterase (AChE) and butyrylcholinesterase (BChE).

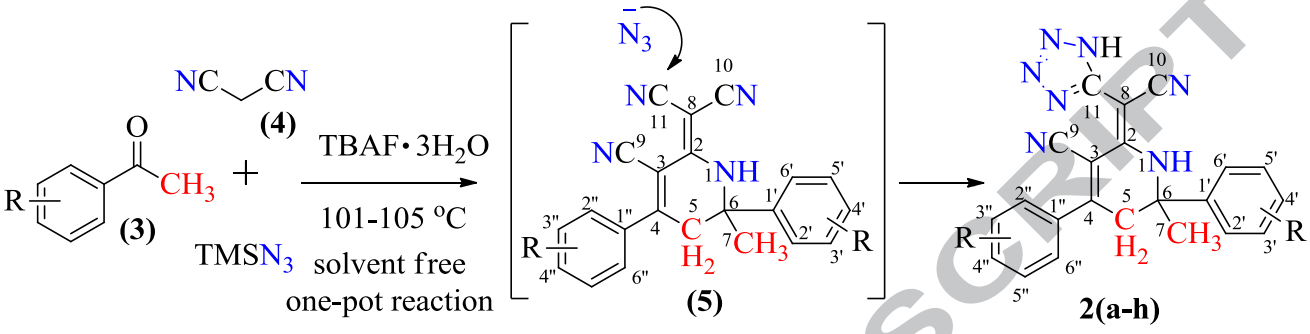

R	Yields (%)	R	Yields (%)
2a, H	(84.8)	**2e**, 3'/3"-Cl	(49.8)
2b, 4'/4"-Me	(53.8)	**2f**, 3'/3"-OMe	(56.8)
2c, 3'/3"-Me	(86.7)	**2g**, 2'/2"-OMe	(65.8)
2d, 4'/4"-F	(47.8)	**2h**, 4'/4"-OH	(70.8)

Scheme-1: One-pot synthesis of tetrazole-1,2,5,6-tetrahydronicotinonitrile **2(a-h)**

2.2 Investigating a plausible reaction mechanism

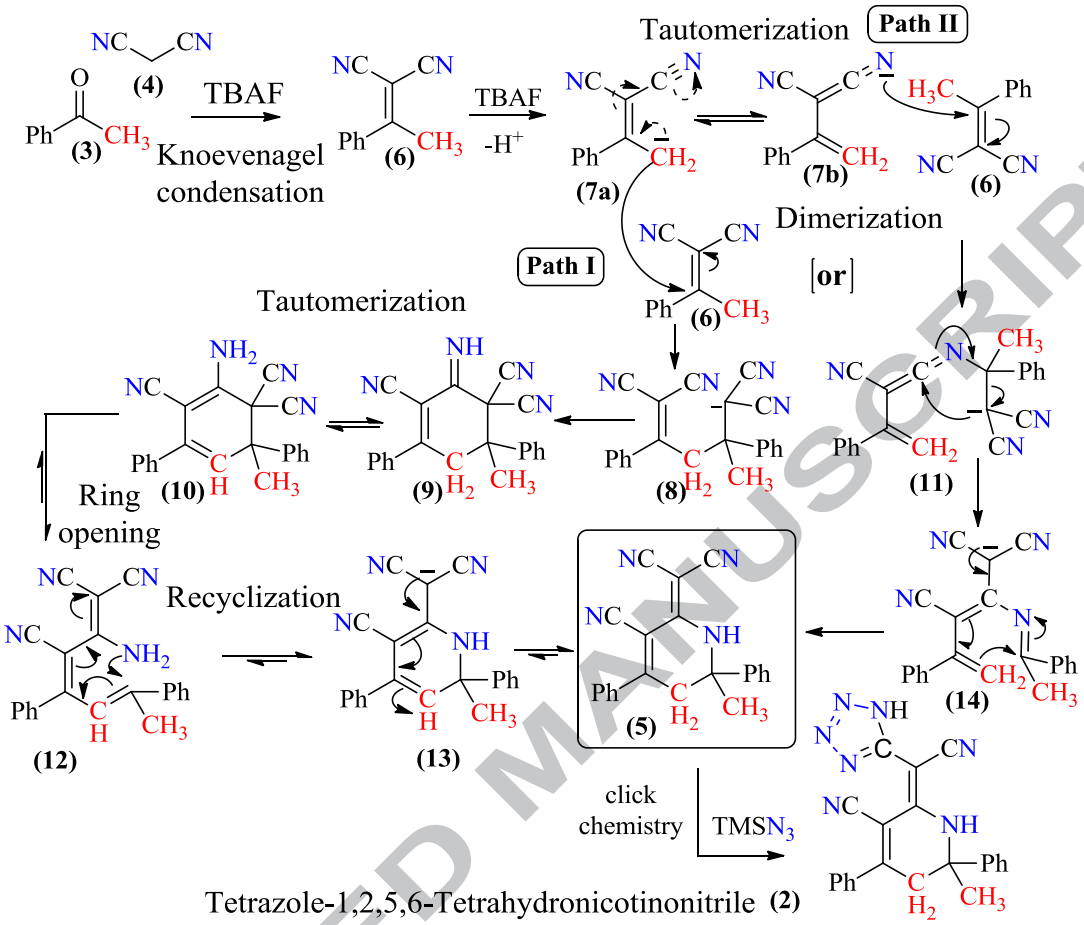

Scheme-2: Plausible pathways **(I)** Michael addition of **(7a)** to **(6),** or **(II)** Dimerization reaction between **(7b)** and **(6)** to yield 1,2,5,6-tetrahydronicotinonitrile **(5)**.

Plausible mechanism of this reaction to form 1,2,5,6-tetrahydronicotinonitrile derivative **(5)** *via* two pathways **(I)** and **(II)**, emanating from intermediate **(7a)** or its tautomer **(7b)**, has been depicted in Scheme-2. The reaction involves a Knoevenagel condensation, followed by a dimerization to afford 1,2,5,6-tetrahydronicotinonitrile **(5)** and click chemistry to form final product **(2)**. Pathway **(I)** suggests Michael addition [5, 19] of carbanion **(7a)** to its neutral species **(6)** followed by ring closure to form cyclohexene **(9)** which could tautomerized to cyclohexadiene **(10)**. It is evident that such type of cyclohexadiene **(10)** is thermally unstable and expeditiously undergoes ring opening to acyclic hexatriene type intermediate **12** [20, 21]. Further, the base (F^-) mediated multistep ring closure generated the dimer **(5)** [19, 22]. In pathway **(II)**, the nucleophilic nitrogen of tautomer **(7b)** attacks arylidenemalononitrile **(6)** to

form intermediate **(11)** which then affords dimer **(5)** *via* intermediate **(14)** (Scheme 2) [2, 23, 24]. Computational studies were preformed to understand plausible mechanism pathway **(I)** or **(II)** for the formation of 1,2,5,6-tetrahydronicotinonitrile **(5)** (see Section-2.3).

The structures of dimer **(5a)** and tetrazole linked 2-dicyanomethylene-6-methyl-4,6-diphenyl-1,2,5,6-tetrahydronicotinonitrile **(2a)**, were fully characterized with different NMR techniques. The compound **(5a)** showed three characteristic signals; a) a broad singlet (brs) for NH^1 proton at δ 9.71 ppm, b) two doublets for each methylene protons H^{5a} and H^{5b} at δ 3.77 and δ 3.30* ppm, respectively, and c) a singlet for C-12 methyl protons at δ 1.71 ppm. The NH^1 proton showed COSY correlation of with H^{5a} and HMBC correlations with C^2, C^3, C^5, C^6, C^7, C^8, C^9 which confirm its position in the structure. In NOSEY spectrum, correlations with H^7 and aromatic $H^{2'}$, $H^{6'}$ were also observed. In COSY spectrum, only H^{5a} methylene proton showed COSY correlation with NH^1. The C^7 methyl proton showed HMBC correlation with $C^{1'}$, C^2, C^4, C^5, C^6 and NOSEY correlation with H^1, $H^{2'}$, H^{5b}, $H^{6'}$. A detail summary of ^{1}H- and C^{13}-NMR and correlation data of compound (**5a)** has been presented in Table-1. While in the case of compound **(2a)** characteristic signals for NH^1 group appears at δ 10.33 ppm in *d*-DMSO, may be deshielding effects due to tetrazole ring. The possible position of tetrazole formation to one of the three nitrile groups (CN-9, CN-10, or C-11) was illustrated by using 2D NMR spectra. In HMBC spectrum, the correlations of C^9 (114.2 ppm) nitrile group with H^{5b} and NH^1 protons confirmed its position. However, the positions of C^{10} and C^{11} nitrile groups in both compounds (**2a** and **5a**) were difficult to assign from NMR data. Therefore, the tetrazole formation at C^{11} position was assigned on the basis of reactivity and availability of CN-11 nitrile group in compound **(5a)**. Some literature showed the addition of nucleophile to such type of synthetic precursor **(5a)** [5, 23]. Moreover, NH^1 group showed HMBC correlations with C^3, C^5, C^6, C^7, and C^8 carbon atoms. Each proton, H^{5a} and H^{5b}, from methylene group (CH_2) group showed doublet at δ 3.77 and 3.30 ppm, respectively. Corresponding correlation data include HMBC, COSY, and NOESY has mentioned in the Table -2. Singlet of C^7 methyl group appears almost at the same position (δ 1.78 ppm) as in the case of **(5a)**. Attempts have also been made to obtain the X-ray crystal structure of compounds in **2(a-h)** series, even with solvent system which has been

*= obscured by H_2O signal in DMSO

used to develop the crystals of **(5a)** [18], were unsuccessful. Therefore, different NMR spectra including 2D data has been discussed and provided in Table-2 to adapt the most favourable structure of compounds in series **2(a-h)**.

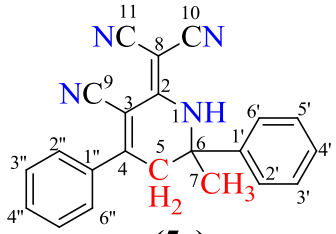

(5a)

Table-1: Characteristic ^{1}H, C^{13} NMR correlation data of **(5a)**

	Atoms No														
	1	**2**	**3**	**4**	**5**		**6**	**7**	**8**	**9**	**10**	**11**	**1'**	**1''**	**2'/2''/3'/3''/4'/4''/5'/5''/6'/6''**
	NH	C	C	C	CH^a	CH^b	C	CH_3	C	CN	CN	CN	C	C	CH x 10 (Aromatic *H*)
δ_H	9.71 (brs)	-	-	-	3.77 (d)	3.30*	-	1.71 (s)	-				-	-	7.58-7.28 (m)
δ_C	-	157.8	101.1	168.9	44.03		56.9	28.2	49.5	113.7	115.5	114.9	142.8	135.5	132.1/128.9/128.6/128.2 /127.5/124.9
HMBC	C^2 C^3 C^5 C^6 C^7 C^8 C^9	-	-	-	$C^{1'}$ $C^{1''}$ C^3 C^4 C^6 C^7	$C^{1'}$ $C^{1''}$ C^2 C^3 C^4 C^6 C^7 C^9	-	$C^{1'}$ C^2 C^4 C^5 C^6	-	-	-	-	-	-	$C^{1'}$ C^2 $C^{2'}C^{3'}$ C^4 $C^{4''}C^{5'}$ $C^{6'}$
COSY	H^{5a}	-	-	-	H^1 H^{5b}	H^{5a}	-	-	-	-	-	-	-	-	$H^{2'}$ $H^{2''}$ $H^{3'}$ $H^{3''}$ $H^{4'}$ $H^{4''}$ $H^{5'}$ $H^{5''}$ $H^{6'}$ $H^{6''}$
NOESY	$H^{2'}$ $H^{6'}$ H^7	-	-	-	$H^{2'}$ H^{5b}	H^{5a}	-	H^1 $H^{2'}$ H^{5b} $H^{6'}$	-	-	-	-	-	-	$H^{2'}$ $H^{2''}$ $H^{3'}$ $H^{3''}$ $H^{4'}$ $H^{4''}$ $H^{5'}$ $H^{5''}$ H^{5a} $H^{6'}$ $H^{6''}$ H^7

*= obscured by H_2O signal in DMSO

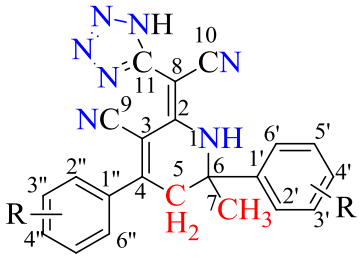

(2a)

Table-2: Characteristic ^{1}H, C^{13} NMR correlation data of **(2a)**

	Atoms No													
	1	**2**	**3**	**4**	**5**		**6**	**7**	**8**	**9**	**10**	**11**	**1'**	**1''**	**2'/2''/3'/3''/4'/4''/5'/5''/6'/6''**
	NH	C	C	C	CH^{a}	CH^{b}	C	CH_3	C	CN	CN	C=N	C	C	CH x 10 (Aromatic *H*)
δ_H	10.33 (brs)	-	-	-	3.77 (d)	3.30*	-	1.71 (s)	-	-	-	-	-	-	7.55-7.29 (m)
δ_C	-	150	102	167	43.9		56.1	29.2	64.1	114.2	116.4	143.4	143.4	136.3	131.6/128.85/128.82/128.1 /127.6/124.9
HMBC	C^3 C^5 C^6 C^7 C^8 C^9	-	-	-	$C^{1''}$ C^3 C^4 C^6	$C^{1'}$ $C^{1''}$ C^3 C^4 C^6 C^7 C^9	-	$C^{1'}$ C^5 C^6	-	-	-	-	-	-	$C^{1'}$ C^2 $C^{2'}$ $C^{3'}$ C^4 $C^{4''}$ $C^{5'}$ $C^{6'}$
COSY	H^{5a}	-	-	-	H^1 H^{5b}	H^{5a}	-	-	-	-	-	-	-	-	$H^{2'}$ $H^{2''}$ $H^{3'}$ $H^{3''}$ $H^{4'}$ $H^{4''}$ $H^{5'}$ $H^{5''}$ $H^{6'}$ $H^{6''}$
NOESY	$H^{2'}$ $H^{6'}$ H^7	-	-	-	$H^{2'}$ H^{5b} H^6 $H^{7'}$	$H^{2'}$ H^{5a} H^6 $H^{7'}$	-	H^1 $H^{2'}$ H^{5a} H^{5b} $H^{6'}$	-	-	-	-	-	-	$H^{2'}$ $H^{2''}$ $H^{3'}$ $H^{3''}$ $H^{4'}$ $H^{4''}$ $H^{5'}$ $H^{5''}$ H^{5a} $H^{6'}$ $H^{6''}$ H^7

*= obscured by H_2O signal in DMSO

2.2 Computational Studies

All calculations were performed by using GAUSSIAN 09 [25]. Geometries of the structures were optimized without any symmetry constraints at hybrid B3LYP (Becke 3-Parameter, Lee, Yang and Parr) method using 6-31G(d) [26-28]. B3LYP is a cost effective method for accurate prediction of geometries of a number of synthetic [29-31] and natural products [32, 33]. Each optimized structure was confirmed by frequency analysis at the same level to confirm the stationary point either as a true minimum (no imaginary frequency) or a transition state (with one imaginary frequency). Intrinsic reaction coordinates (IRC) calculations were performed to confirm that the transition states connect to the right starting materials and products. IRC was performed until the stationary point was reached with RMS gradient less than 1×10^{-4}. The stationary points located through IRC were then completely optimized at the above mentioned method. The reported energies for all structures are in kcal mol^{-1} and include unscaled zero point energy corrections.

Density Functional Theory (DFT) calculations have been performed to explore possible reaction mechanism for the formation of **(5)** from **(6)** and **(7)**. The first step involves Knoevenagel condensation in which active hydrogen of **(4)** undergoes nucleophilic addition to a carbonyl group resulting in dehydration reaction to produce intermediate **(6)**. The intermediate **(6)** has an acidic proton which is abstracted by a mild base (TBAF) to generate the intermediate **(7)** (exists in two tautomeric forms (**7a** and **7b**). Condensation of **(7a)** or **(7b)** with **(6)** leads to two different mechanistic pathways for the synthesis of 1,2,5,6-tetrahydronicotinonitrile; 1) Michael addition (Path I) and 2) Dimerization reaction (Path II, Scheme-2).

In the Michael addition reaction, active methylene carbon (CH_2) of intermediate **(7a)** adds to electrophilic carbon of intermediate **(6)** in a 1,4-addition manner (Figure-2a). The Michael addition is kinetically and thermodynamically highly favorable. The reaction takes place without any activation barrier. A transition state is located at a lower energy compared to the reactants (-0.06 kcal mol^{-1}). The bond distance among both joining carbons is 2.14 Å (Figure-2). The small negative activation barrier is within the error limits of the DFT method applied here. Therefore, it can be concluded safely that the process is virtually barrier less. The reaction is thermodynamically favorable by 4 kcal mol^{-1}; the products are more stable than the reactants.

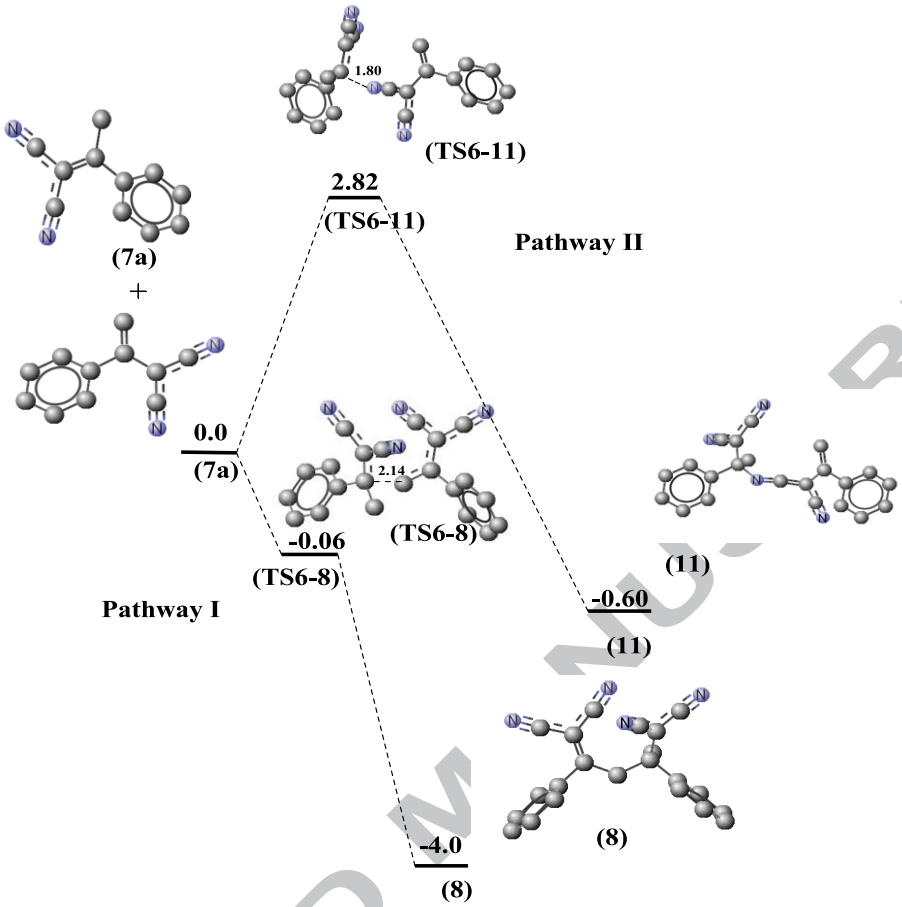

Figure-2: Energy profile of Michael addition and Dimerization reaction of **(7a)** and **(6)**, calculated at B3LYP/6-31G(d). All energies are relative to **(7a),** hydrogen atoms have been removed for clarity. Bond lengths and bond angles are shown in Angstroms and degrees, respectively.

An alternative mechanism proposed for the reaction of **(7b)** with **(6)** is the dimerization reaction, where two monomers **(7b)** and **(6),** join together to form covalently bonded intermediate **(11)**. The nucleophilic nitrogen of intermediate **(7b)** attacks the electrophilic carbon of intermediate **(6)** (Scheme-2). Transition state **(TS6-11),** for the dimerization reaction, is located at a higher energy (2.82 kcal mol^{-1}) from the reactants. The dimerization reaction is also a kinetically and thermodynamically favorable process. The activation barrier for **(TS6-11)**, although higher than the competitive **(TS6-8)**, is still negligible, and easily accessible under the reaction conditions. The joining nitrogen and carbon atoms are at a distance of 1.80 Å in the transition state.

Since, the activation barriers for both reactions (Michael addition and dimerization reactions) are easily accessible at room temperature; therefore, these initial steps don't deliver any concluding information regarding the selective operation of any mechanism. We believe that the subsequent steps may play decisive role therefore, activation barrier for the subsequent steps are also analyzed and discussed below.

Path I

In path I, The intermediate **(8)** undergoes ring closure through transition state **(TS8-9)** resulting in the generation of intermediate **(9)** (Figure-3). The nucleophilic attack of electron rich carbon of **(7)** on the electrophilic nitrile group is again a kinetically favorable process. The activation barrier is 14.72 kcal mol^{-1}, which is easily accessible under the reaction conditions. This activation energy is higher as compared to the first step **(TS6-8)**, mainly due to the bulky groups attached to both carbons that undergo reaction. The bond distance between the joining atoms is 2.07 Å which confirms the bond formation among two carbons to form a cyclohexene structure **(9)**.

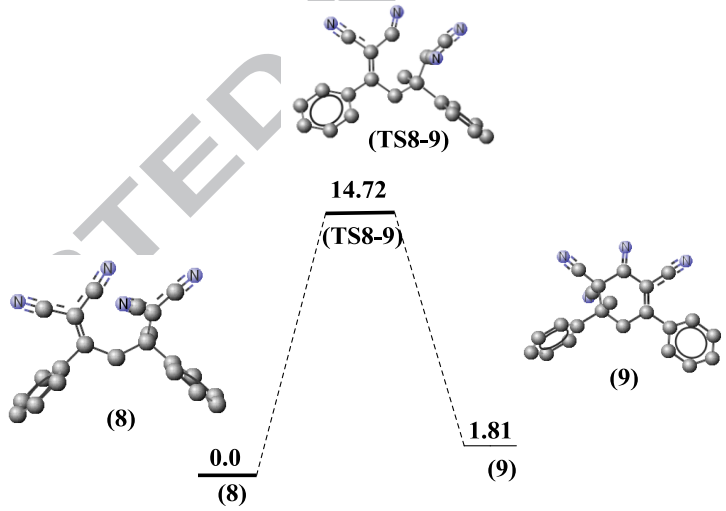

Figure-3: Energy profile of generation of intermediate **(9)** from **(8)**, calculated at B3LYP/6-31G(d). The energies are relative to **(8)** at 0.0 kcal mol^{-1}, hydrogen atoms have been removed for clarity.

The intermediate **(9)** undergoes tautomerization to deliver cyclohexadiene **(10)** which is thermally unstable and undergoes ring opening to acyclic hexatriene type intermediate **(12)** through transition state **(TS10-12)** (Figure-4). Activation energy for the reaction is calculated to

be 19.93 kcal mol^{-1} that show reaction feasibility. The bond distance, in the transition state, among the two carbons is 2.39 Å which shows bond breakage of the cyclic structure.

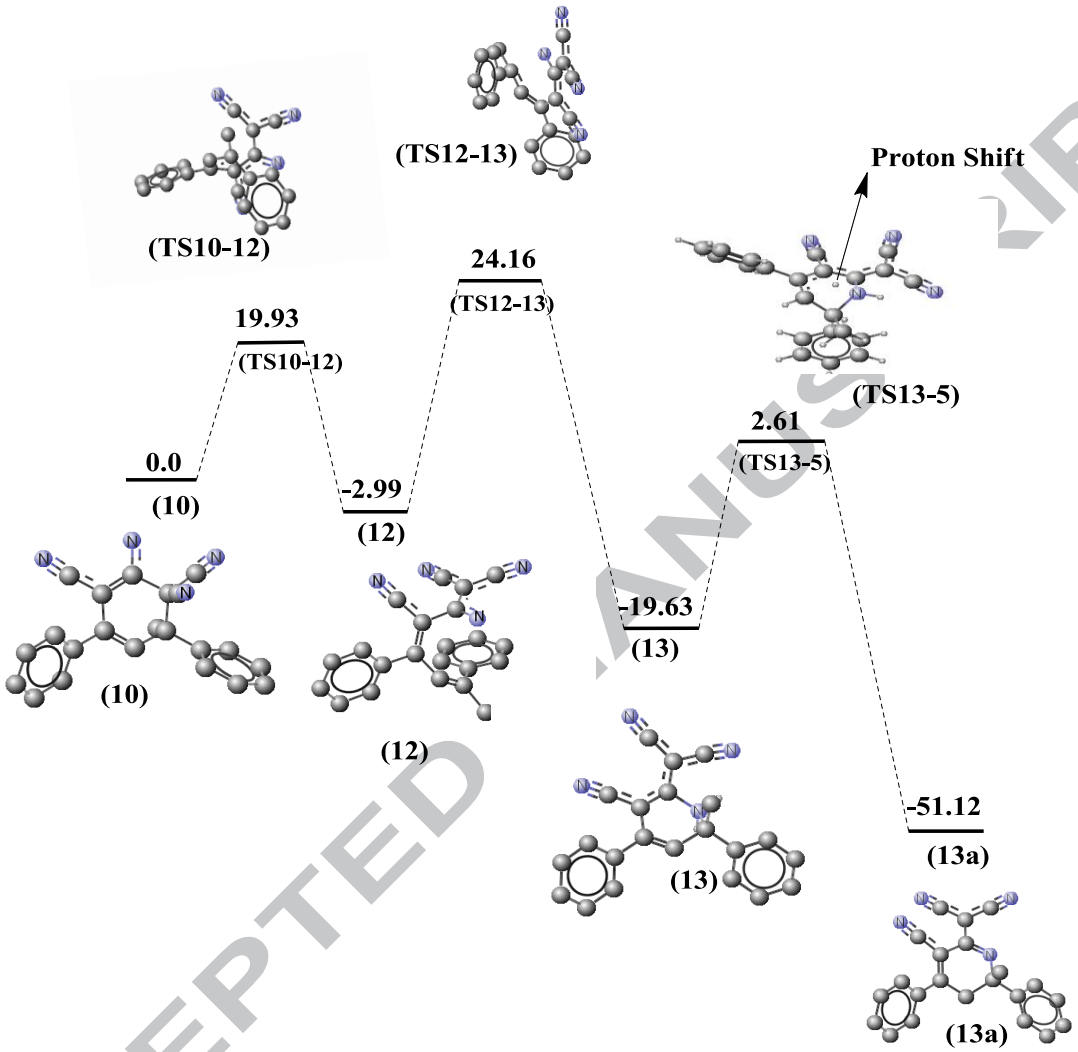

Figure-4: Energy profile for the conversion of **(10)** into **(13a)** through a cascade of electrocyclization and proton transfer, calculated at B3LYP/6-31G(d), hydrogen atoms have been removed for clarity. All energy values are relative to **(10)** at 0.0 kcal mol^{-1}.

In the next step recyclization reaction takes place in which electrocyclization involves NH_2 moiety incorporated in the hexatriene moiety undergoing electrocyclization. The C-N bond distance is 2.07 Å in the transition state **(TS 12-13)** (Figure-5) and the activation energy for the reaction is 24.69 kcal mol^{-1}. The intermediate **(13)** undergoes sigmatropic 1,3-shift of hydrogen between the nitrogen and carbon of the closed ring followed by formation of ionic product **(13a)**

which on protonation will convert to final 1,2,5,6-tetrahydronicotinonitrile **(5)** (Figure-4). The reaction proceeds with an activation energy 27.15 kcal^{-1}. The activation barrier is relatively high but still accessible under reaction conditions (100 $^{\circ}$C). The proton shift can alternatively take place by a low energy pathway involving intermolecular proton shift where the activation barrier is generally about 10-12 kcal mol^{-1}.

In pathway II, the arylidenemalononitrile **(6)**, underwent dimerization reactions *via* tautomer **(7b)** to generate intermediate **(11)**. The intermediate **(11)** can undergo 1,3-sigmatropic shift of $CH(CN)_2$ group to deliver the intermediate **(14)**; however, all attempts to locate the transition state for such transformation met with failure. This sigmatropic shift is not believed to be a low energy process because such sigmatropic shifts are kinetically highly unfavorable (activation barriers are generally more than 40 kcal mol^{-1}). Therefore an alternative mechanism is proposed where intermediate **(11)** first cyclizes to produce intermediate **(15)** (with a cyclobutane moiety) which opens up at another position to deliver intermediate **(14)**. The carbanion of intermediate **(11)** undergoes intramolecular nucleophilic attack on the electrophilic carbon to deliver cyclized product **(15)**. The **(TS11-15)** shows the formation of a four membered ring which is responsible for the formation of intermediate **(15)** (Figure-5).

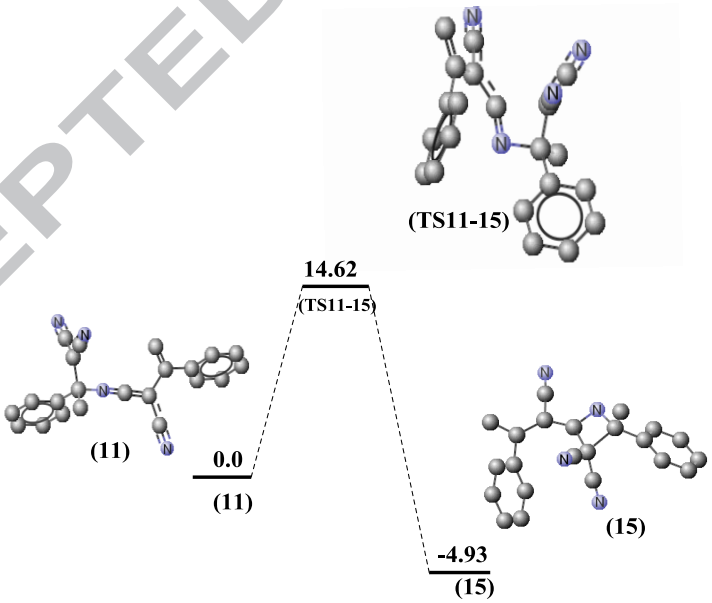

Figure-5: Energy profile of generation of **(15)** from **(11)**, calculated at B3LYP/6-31G(d), hydrogen atoms have been removed for clarity. All energies are relative to **(11)** at 0.0 kcal mol^{-1}.

Opening of cyclobutane ring of intermediate **(15)** occurs in the next step in which transition state **(TS15-14)** (Figure-6) shows the loosening of bond between two carbons. The C-C bond length is 2.22 Å in the transition state which was 1.58 Å in Intermediate **(15)**. The reaction proceeds with an activation energy of 11.01 kcal mol^{-1}. Both cyclization (to produce a cyclobutane ring in intermediate **15**) and then opening of the ring (to produce intermediate **14**) are kinetically favorable processes, and the activation barriers are easily accessible under the reaction conditions. Finally, Intermediate **(14)** undergoes cyclization reaction with an activation barrier of 11.43 kcal mol^{-1} to deliver the final product **(5)** after the protonation of intermediate **(13a)**. The calculated kinetic barriers and thermodynamics associated with reactions for Path **(I)** and **(II)** are easily accessible under the reaction conditions; therefore, it can be concluded that both mechanisms are operational under the reaction conditions.

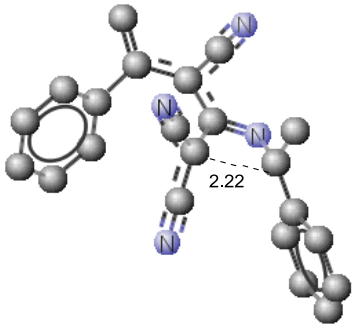

Figure-6: structure of transition state **(TS15-14)**, calculated at B3LYP/6-31G(d), hydrogen atoms have been removed for clarity. Bond length is in Angstroms.

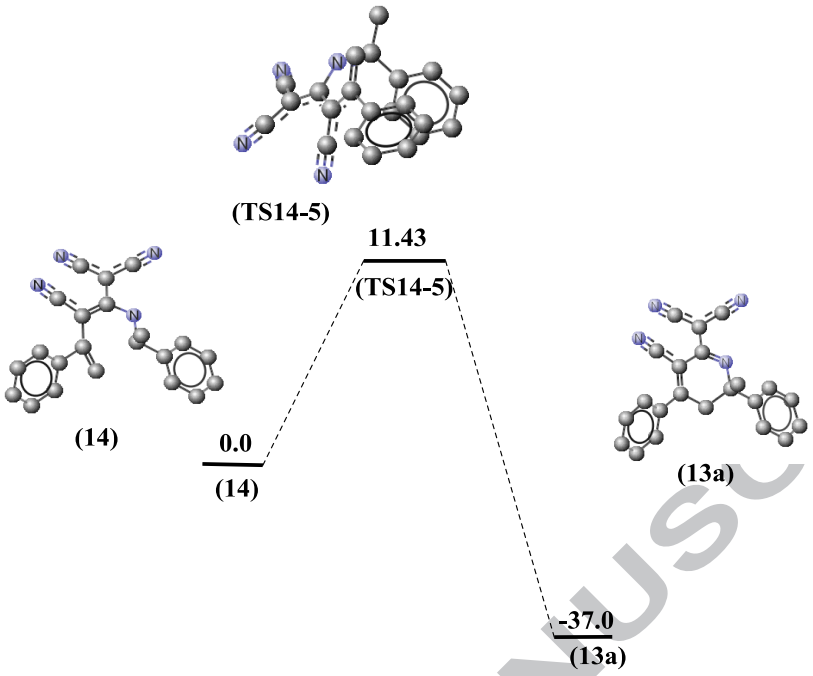

Figure-7: Energy profile for generation of ionic product **(13a)** from **(14)** through elelctrocyclization, calculated at B3LYP/6-31G(d), hydrogen atoms have been removed for clarity.

2.3 Bioactivity and Structure Activity Relationship (SAR)

All successfully synthesized tetrazole linked 1,2,5,6-tetrahydronicotinonitriles **2(a-h)** were evaluated for their anticholinesterase activities against AChE and BChE, which were obtained from *electric eel* and equine serum, respectively, by using Ellman's assay [34]. The previously reported 1,2,5,6-tetrahydronicotinonitriles **5(a-h)** [18] were also evaluated for cholinesterase inhibition. The bioactivity results of the both series tetrazole linked 1,2,5,6-tetrahydronicotinonitriles **2(a-h)** and its precursors **5(a-h)** demonstrated that mostly compounds were active against both AChE and BChE compared to standard inhibitors *i.e.* neostigmine and donepezil (Table-3). From the bioactivities data, 4'/4"-fluoro **(2d)** derivatives was found to exhibited highest inhibitory activity for AChE with IC_{50} values of and 2.01 ± 0.027 μM while the 2'/2"-methoxy derivative **(2g)** revealed highest inhibitory activity in submicromolar level for BChE with IC_{50} value of 0.290 ± 0.130 μM. Limited SAR suggested that the activity of these compounds depend on the nature of substitution and its position on the phenyl rings belong to acetophenone.

In 1,2,5,6-tetrahydronicotinonitriles **5(a-h)** series, all compounds displayed better AChE inhibitory activity as compared to BChE inhibitory activity (Table 1). The 3'/3''-methoxy derivative **(5g)** exhibited highest activity with IC_{50} value of 1.62 ± 0.041 μM against AChE, which indicated the importance of substituent pattern on phenyl ring during enzyme inhibition. On the other hand, among the tetrazole linked 1,2,5,6-tetrahydronicotinonitriles **2(a-h)**, the inhibitory activity was also varies due to different substituent pattern on the phenyl ring. The derivative **(2a)** without any substituents was found moderately active only against AChE with IC_{50} values of 7.02 ± 0.19 μM. The 4'/4''-methyl substituted derivative **(2b)** showed inhibition potential against both AChE and BChE with IC_{50} value 4.45 ± 0.180 μM and 5.87 ± 0.128 μM, respectively, while the 3'/3''-methyl derivative **(2c)** which was found poorly or almost inactive against both enzymes (Table-1). In halogen compounds, the derivative **(2d)** was found more active against AChE than BChE while the 3'/3''-chloro analogue **(2e)** acted as potent dual inhibitor for AChE with IC_{50} value of 2.32 ± 0.091 μM and as well as for BChE with IC_{50} values of 2.78 ± 0.216 μM. The 4'/4''-hydroxy derivative **(2h)** with IC_{50} value of 7.42 ± 0.489 μM showed moderate activity against AChE, whereas it displayed significant activity against BChE with an IC_{50} value of 2.45 ± 0.30 μM. In the case of methoxy derivatives, the 3'/3''-methoxy derivative **(2f)** showed selectively moderate inhibitory activity with IC_{50} values of 5.11 ± 0.12 μM for only AChE, while the 2'/2''-methoxy derivative **(2g)** displayed excellent inhibitory activity with IC_{50} values of 0.290 ± 0.130 μM (Table 1). The above described results strongly suggested that substituent's electronic effect and position on phenyl ring influenced the inhibitory activity of compounds.

Table-3: *In Vitro* AChE and BChE inhibition activities of 1,2,5,6-tetrahydronicotinonitrile **5(a-h)** and tetrazole linked derivatives **2(a-h)**.

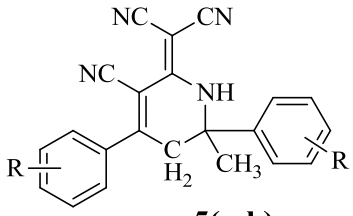

5(a-h)

	Compounds	AChE	BChE	Selectivity[b]
	R	IC_{50}[a] (μM)		
5a	H	20.3 ± 0.481	48.1 ± 0.691	2.37
5b	4′/4″-Methyl	16.9 ± 0.95	36.5 ± 1.19	2.16
5c	3′/3″-Methyl	5.21 ± 0.092	35.9 ± 1.54	6.89
5d	4′/4″-Fluoro	11.9 ± 0.420	55.2 ± 0.89	4.64
5e	4′/4″-Iodo	11.2 ± 0.401	45.3 ± 2.581	4.04
5f	3′/3″-Fluoro	8.01 ± 0.201	68.8 ± 1.98	8.59
5g	3′/3″-Methoxy	1.56 ± 0.041	48.2 ± 1.96	30.9
5h	4′/4″-Hydroxy	5.38 ± 0.125	42.2 ± 0.070	7.84

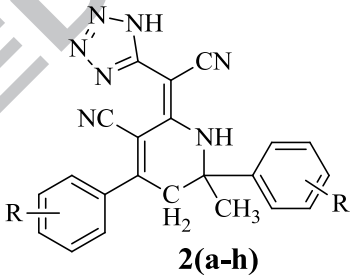

2(a-h)

2a	H	7.02 ± 0.19	22.1 ± 1.40	3.14
2b	4′/4″-Methyl	4.45 ± 0.180	5.87 ± 0.128	1.31
2c	3′/3″-Methyl	20.8 ± 0.582	62.2 ± 0.80	2.30
2d	4′/4″-Fluoro	2.01 ± 0.027	38.8 ± 0.98	19.3
2e	3′/3″-Chloro	2.32 ± 0.091	2.78 ± 0.216	1.19
2f	3′/3″-Methoxy	5.11 ± 0.12	39.2 ± 1.58	7.67
2g	2′/2″-Methoxy	20.3 ± 0.861	0.290 ± 0.130	0.014
2h	4′/4″-hydroxy	7.42 ± 0.489	2.45 ± 0.30	0.33

Neostigmine[c]	19.3 ± 3.21	43.2 ± 4.21	2.23
Donepezil[c]	0.019 ± 0.002	8.41 ± 0.381	442

[a] Inhibitory concentration; [b] Selectivity ratio = IC_{50} ratio (BChE/AChE); [c] Standard inhibitors for cholinesterase activities

3. Conclusion

In conclusion, one-pot solvent-free synthesis of tetrazole linked 1,2,5,6-tetrahydronicotinonitrile derivatives **5(a-h)** has been carried out in the presence of TBAF. Two plausible reaction mechanisms **(I)** and **(II)** (Scheme 2) were elaborated by using DFT calculations which demonstrated pathway **(I)** to be the most feasible one. Moreover, bioactivity studies of 1,2,5,6-tetrahydronicotinonitriles **5(a-h**) and tetrazole linked derivatives **2(a-h**) were performed against cholineresatease, AChE and BChE. In most of the cases, tetrazole linked 1,2,5,6-tetrahydronicotinonitriles **2(a-h)** were found more active than intermediates **5(a-h)**. The tetrazole analogue **(2g)** was found a potent selective inhibitor with IC_{50} values of 0.290 ± 0.130 μM against BChE, which has elevated activity in AD brain, as compared to reference inhibitors, neostigmine and donepezil. The compound **(2g)** could be potentially served as lead for further structural modifications in order to enhance potency and selectivity against cholinesterase to affect AD symptoms.

4. Material and Methods (Chemistry)

The starting materials which include the different derivatives of acetophenone (≥99%), malononitrile (≥99%), and tetrabutylammonium fluoride trihydrated (TBAF) (98%) were purchased from Sigma-Aldrich and used without any purification unless otherwise stated. The reagent grade ethyl acetate, diethyl ether, hexane, HCl laboratory grade and distilled water were used as solvents during reaction workup and purification. All the reactions were performed in screw capped Micro Reaction Vessels (5 mL), purchased from Sigma-Aldrich. Thin layer chromatography (TLC) was used to monitor reaction using silica gel 60 aluminium-backed plates 0.063-0.200 mm as the stationary phase with analytical grade solvents such as ethyl acetate (EtOAc), diethyl ether, *n*-hexane etc. Chromatograms were visualized with UV light (254 nm) or using different staining mixtures such as basic potassium permanganate, vanillin, ninhydrin and bromocresol green. Infrared spectra IR (KBr discs) were recorded between 4000-500 cm^{-1} on a Bruker Vector-22 spectrometer. TGA and DSC analyses were carried out on a TA instrument, model number SDT Q600. Aluminum heating/sample pans were used. The sample weight used

was 3-6 mg. Decomposition profiles were obtained at four different constant heating rates, that is, 5 °C/min, 10 °C/min, 15 °C/min and 20 °C/min. All analyses were carried out under nitrogen atmosphere (flow rate was 100 ml/min). The data were processed by use of Universal Analysis 2000 software, version 4.2E (TA Instruments, USA), and MS Excel 2013. Bruker spectrometers were used to record ^{1}H NMR spectra at 300, 400 or 500 MHz and ^{13}C NMR at 75, 100 or 125 MHz as dilute solutions in the appropriate deuterated solvent at 25 °C.

All the chemical shifts were recorded on the *δ*-scale (ppm) using residual solvents as an internal standard (DMSO; ^{1}H 2.50, ^{13}C 39.43 and $CHCl_3$; ^{1}H 7.26, ^{13}C 77.16). Coupling constant were calculated in Hertz (Hz) and multiplicities were labelled s (singlet), d (doublet), t (triplet), q (quartet), quint (quintet) and the prefixes br (broad) or app (apparent) were used. Mass spectra (ESI^+) were recorded at Finnigan MAT-321A, Germany by using electrospray (ES+), electron impact (EI+ EI+) or FAB (Fast atom bombardment) techniques. Melting points of solids were determined using a Stuart™ melting point apparatus SMP3 apparatus and are uncorrected. Butyrylcholinesterase (BuChE) (EC 3.1.1.8, from horse serum), acetylcholinesterase (AChE) (EC 3.1.1.7, type VI-S from electric eel), *S*-butyrylthiocholine chloride (BTCCl), acetylthiocholine iodide (ATCI), 5,5'-dithio-*bis*(2-nitrobenzoic acid) (DTNB), neostigmine methylsulphate and dimethylsulphoxide (DMSO) and donepezil hydrochloride were purchased from Sigma-Aldrich (St. Louis, MO, USA).

5.1 General procedure for the synthesis of 1,2,5,6-Tetrahydronicotinonitrile Derivatives 2(a-h)

In a general procedure, an oven dried sealed vessel was charged with the corresponding acetophenone (1.0 mmol), malononitrile (1.5 mmol) and TBAF (1.0 mmol) at room temperature. The reactions were then heated at 100-103 °C with constant stirring until the complete consumption of the starting material, monitored by TLC analysis. At this reaction stage, trimethylsilyl azide (1.0 mmol) was added into the same sealed vessel and left the resulting mixture for further stirring at 100-103 °C for 3-4 hr. The reaction mixture was cooled to room temperature, poured in to 10% HCl to remove TBAF and extracted with EtOAc. The organic layer was dried with $MgSO_4$, filtered and evaporator on rotary evaporator. The crude product was purified by silica gel column chromatography with 80% EtOAc in hexane to afford the desired pure compounds **2(a-h)** in different yields (Figure 2). The structures of each compound

2(a-h) were confirmed with NMR, IR spectroscopy and mass spectrometry. The structures of each compound **2(a-h)** were confirmed with NMR, IR spectroscopy and mass spectrometry. The spectral data of all compounds **5(a-h)** was reported previously reported [18].

5.2 Spectral data compounds

2-Dicyanomethylene-6-methyl-4,6-bis(phenyl)-1,2,5,6-tetrahydronicotinonitrile (5a) [18]
^{1}H and C^{13} NMR (Table-1); EI-HRMS calculated for $C_{22}H_{16}N_4$ (M): 336.1375, Found: 336.1355; Anal. calcd for $C_{24}H_{20}N_4O_2$; C, 78.55; H, 4.79; N, 16.66 found: C = 78.24, H = 4.99, N = 16.99%.

2-(Cyano(1*H*-tetrazol-5-yl)methylene)-6-methyl-4,6-bis(phenyl)-1,2,5,6-tetrahydronicotinonitrile (2a)
Brown solid (334 mg, 84.8%), mp 166 $^{\circ}C$, ^{1}H and C^{13} NMR (Table-2); HRMS (ESI) calculated for $C_{22}H_{18}N_7$: 380.1623 $(M+H)^+$, Found: 380.1596.

2-(Cyano(1*H*-tetrazol-5-yl)methylene)-6-methyl-4,6-bis(4′/4′′-methylphenyl)-1,2,5,6-tetrahydronicotinonitrile (2b)
Following the general procedure, the corresponding 1,2,5,6-tetrahydronicotinonitrile derivative **(2b)** was isolated as a yellow solid (224 mg, 53.8%). mp 201 $^{\circ}C$; υ_{max} /cm^{-1} (KBr solid) 3429, 3138, 2923, 2203 (CN), 2138, 1733, 1606, 1542, 1446, 1408, 1380, 1190; ^{1}H NMR (300 MHz, DMSO) δ_H 10.30 (1H, brs, NH), 7.41 (2H, d, *J* 8.1 Hz, Ar*H*), 7.33 (4H, d, *J* 8.4 Hz, Ar*H*), 7.18 (2H, d, *J* 8.1 Hz, Ar*H*), 3.74 (1H, d, *J* 18.6 Hz, C*H*^{5a}H^{5b}), 3.32 (1H, d, CH^{5a}*H*^{5b}, obscured by H_2O in DMSO), 2.36 (3H, s, Ar*CH*$_3$), 2.26 (3H, s, Ar*CH*$_3$), 1.74 (3H, s, CH_3); ^{13}C NMR (75 MHz, DMSO) δ_C 166.9, 150.4, 142.1, 140.4, 136.7, 133.2, 129.4, 129.3, 128.3, 124.7, 116.4, 114.5, 101.1, 64.1, 55.9, 43.7 (CH_2), 29.2 (CH_3), 20.9 (CH_3), 20.4 (CH_3); HRMS (ESI) calculated for $C_{24}H_{22}N_7$: 408.1936 $(M+H)^+$, Found: 408.1903.

2-(Cyano(1*H*-tetrazol-5-yl)methylene)-6-methyl-4,6-bis(3′/3′′-methylphenyl)-1,2,5,6-tetrahydronicotinonitrile (2c)
Following the general procedure, the corresponding 1,2,5,6-tetrahydronicotinonitrile derivative **(2c)** was isolated as a brown solid (360 mg, 86.7%). mp 202 $^{\circ}C$; υ_{max} /cm^{-1} (KBr solid) 3456, 3130, 3045, 2922, 2206 (CN), 1606, 1558, 1450, 1380, 1274, 1043; ^{1}H NMR (300 MHz, DMSO) δ_H 10.25 (1H, brs, NH), 7.43-7.33 (3H, m, Ar*H*), 7.30-7.24 (3H, m, Ar*H*), 7.20 (1H, app

d, *J* 8.0 Hz, Ar*H*), 7.11 (1H, d, *J* 7.2 Hz, Ar*H*), 3.73 (1H, d, *J* 18.4 Hz, C*H*^{5a}H^{5b}), 3.32 (1H, d, CH^{5a}*H*^{5b}, obscured by H_2O in DMSO), 2.35 (3H, s, Ar*CH*$_3$), 2.31 (3H, s, Ar*CH*$_3$), 1.77 (3H, s, CH_3); ^{13}C NMR (75 MHz, DMSO) δ_C 167.4, 150.5, 143.2, 138.2, 138, 136.4, 132.2, 128.7, 128.6, 128.5, 128.2, 125.6, 126.3, 121.9, 116.6, 114.2, 101.9, 64, 56.1, 44 (CH_2), 29.1 (CH_3), 21.1 (CH_3), 20.8 (CH_3); HRMS (ESI) calculated for $C_{24}H_{22}N_7$: 408.1936 $(M+H)^+$, Found: 408.1919.

2-(Cyano(1*H*-tetrazol-5-yl)methylene)-6-methyl-4,6-bis(4′/4′′-fluorophenyl)-1,2,5,6-tetrahydronicotinonitrile (2d)

Following the general procedure, the corresponding 1,2,5,6-tetrahydronicotinonitrile derivative **(2d)** was isolated as a brown solid (360 mg, 47.8%). mp 170 $^{\circ}$C; υ_{max} /cm^{-1} (KBr solid) 3371, 3236, 2924, 2858, 2205 (CN), 1606, 1556, 1479, 1387, 1276, 1068, 1002; ^{1}H NMR (300 MHz, DMSO) δ_H 10.29 (1H, each brs, NH), 7.91 (2H, d, *J* 8.4 Hz, Ar*H*), 7.73 (2H, d, *J* 8.4 Hz, Ar*H*), 7.24 (4H, t, *J* 8.2 Hz Ar*H*), 3.76 (1H, d, *J* 18 Hz, C*H*^{5a}H^{5b}), 3.36 (1H, d, CH^{5a}*H*^{5b}, obscured by H_2O in DMSO), 1.78/1.71 (3H, each s, CH_3); ^{13}C NMR (75 MHz, DMSO) δ_C 165.8, 165, 164.4, 162.57/162.54, 160.2, 154.2, 149.8, 139.4, 130.9/130.8, 127.2/127.1, 116.2, 116.1/115.9, 115.6/115.4, 114, 102, 64.2, 55.8, 43.9 (CH_2), 29.1 (CH_3); HRMS (ESI) calculated for $C_{22}H_{16}F_2N_7$: 416.1435 $(M+H)^+$, Found: 416.1438.

2-(Cyano(1*H*-tetrazol-5-yl)methylene)-6-methyl-4,6-bis(3′/3′′-chlorophenyl)-1,2,5,6-tetrahydronicotinonitrile (2e)

Following the general procedure, the corresponding 1,2,5,6-tetrahydronicotinonitrile derivative **2e** was isolated as a brown solid (224 mg, 49.8%). mp 152 $^{\circ}$C; υ_{max} /cm^{-1} (KBr solid) 3400, 2924, 2206 (CN), 1609, 1568, 1514, 1415, 1269, 1080, 1029; ^{1}H NMR (400 MHz, DMSO) δ_H 10.23 (1H, brs, NH), 7.63 (2H, app d, *J* 8.0 Hz, Ar*H*), 7.57 (1H, t, *J* 7.8 Hz, Ar*H*), 7.48 (1H, brs, Ar*H*), 7.43 - 7.33 (4H, m, Ar*H*), 3.78 (1H, d, *J* 18.4 Hz, C*H*^{a}H^{b}), 3.38 (1H, d, CH^{a}*H*^{b}, obscured by H_2O in DMSO), 1.79 (3H, s, CH_3); ^{13}C NMR (100 MHz, DMSO) δ_C 165.2, 149.4, 147.5, 145.9, 138.1, 133.7, 133.5, 131.2, 130.8, 130.7, 127.8, 127.7, 127.6, 125.2, 123.8, 116, 113.6, 103 1, 64.1, 56, 43.5 (CH_2), 28.5 (CH_3); HRMS (ESI) calculated for $C_{22}H_{15}Cl_2N_7$: 448.0844 $(M+H)^+$, Found: 448.0849.

2-(Cyano(1*H*-tetrazol-5-yl)methylene)-6-methyl-4,6-bis(3′/3′′-methoxyphenyl)-1,2,5,6-tetrahydronicotinonitrile (2f)

Following the general procedure, the corresponding 1,2,5,6-tetrahydronicotinonitrile derivative **(2f)** was isolated as a brown solid (141 mg, 56.8%). mp 173 $^{\circ}$C; υ_{max} /cm^{-1} (KBr solid) 3414, 3233, 2836, 2205 (CN), 1642, 1603, 1542, 1488, 1457, 1430, 1380, 1290, 1257, 1174, 1041; ^{1}H NMR (300 MHz, DMSO) δ_H 10.28 (1H, brs, NH), 7.43 (1H, t, *J* 7.8 Hz, Ar*H*), 7.32 (1H, t, *J* 8 Hz, Ar*H*), 7.11 (1H, dd, *J* 2, 8.4 Hz, Ar*H*), 7.04 (1H, d, *J* 9.2 Hz, Ar*H*), 7.03 (1H, brs, Ar*H*), 6.99 (1H, d, *J* 8 Hz, Ar*H*), 6.93 (1H, brs, Ar*H*), 6.88 (1H, dd, *J* 2, 8.4 Hz, Ar*H*), 3.79 (3H, s, ArO*CH*$_3$), 3.73 (1H, d, *J* 18.4 Hz, C*H*^{5a}H^{5b}), 3.73 (3H, s, ArO*CH*$_3$), 3.30 (1H, d, CH^{5a}*H*^{5b}, obscured by H_2O in DMSO), 1.78 (3H, s, CH_3). ^{13}C NMR (125 MHz, DMSO) δ_C 167.1, 159.9, 158.8, 147.8, 142.7, 140.6, 133.2, 130.7, 129.7, 121.8, 116.5, 116.2, 116, 115.1, 113.8, 114.2, 110.5, 102.1, 65.2, 56.2, 55.2 (OCH_3), 55 (OCH_3), 43.8 (CH_2), 28.9 (CH_3); HRMS (ESI) calculated for $C_{24}H_{22}N_7O_2$: 440.1834 $(M+H)^+$, Found: 440.1807.

2-(Cyano(1*H*-tetrazol-5-yl)methylene)-6-methyl-4,6-bis(2′/2′′-methoxyphenyl)-1,2,5,6-tetrahydronicotinonitrile (2g)

Following the general procedure, the corresponding naphthyridine derivative **(2g)** was isolated as a brown solid (295 mg, 65.8%). mp 171 $^{\circ}$C; υ_{max} /cm^{-1} (KBr solid) 3474, 3414, 3234, 2936, 2839, 2202 (CN), 1612, 1556, 1488, 1461, 1435, 1291, 1254, 1164, 1023; ^{1}H NMR (300 MHz, DMSO) δ_H 10.46 (1H, brs, NH), 7.48 (1H, t, *J* 7.6 Hz, Ar*H*), 7.33 (1H, t, *J* 7.6 Hz, Ar*H*), 7.14 (2H, dd, *J* 8.8, 11.6 Hz, Ar*H*), 7.06-6.99 (3H, m, Ar*H*), 6.92 (1H, t, *J* 7.2 Hz Ar*H*), 3.83 (3H, s, ArO*CH*$_3$), 3.74 (3H, s, ArO*CH*$_3$), 3.78 (1H, d, *J* 25.5 Hz, C*H*^{5a}H^{5b}), 3.32 (1H, d, CH^{5a}*H*^{5b}, obscured by H_2O in DMSO), 1.80 (3H, s, CH_3); ^{13}C NMR (75 MHz, DMSO) δ_C 166.3, 156.4, 156.1, 149.2, 132.3, 129.44, 129.38, 128.6, 126.07, 125.96, 120.54, 120.50, 116.3, 113.6, 112.4, 112.1, 103.7, 65.2, 55.8, 55.6 (OCH_3), 55.5 (OCH_3), 41.2 (CH_2), 26.3 (CH_3); HRMS (ESI) calculated for $C_{24}H_{22}N_7O_2$: 440.1834 $(M+H)^+$, Found: 440.1805.

2-(Cyano(1*H*-tetrazol-5-yl)methylene)-6-methyl-4,6-bis(4′/4′′-hydroxyphenyl)-1,2,5,6-tetrahydronicotinonitrile (2h)

Following the general procedure, the corresponding naphthyridine derivative **(2h)** was isolated as a brown solid (209 mg, 70.8%). mp 130 $^{\circ}$C; υ_{max} /cm^{-1} (KBr solid) 3357, 2924, 2208 (CN), 1639, 1569, 1512, 1440, 1381, 1267, 1232, 1172, 1109, 1034; ^{1}H NMR (400 MHz, DMSO) δ_H 10.71

(1H, s, ArO*H*) 10.15 (1H, brs, NH), 9.33 (1H, s, ArO*H*), 7.37 (2H, d, *J* 8.8 Hz, Ar*H*), 7.17 (2H, d, *J* 8.4 Hz, Ar*H*), 6.83 (2H, d, *J* 8.4 Hz, Ar*H*), 6.69 (2H, d, *J* 8.4 Hz Ar*H*), 3.53 (1H, d, *J* 17.6 Hz, C*H*^{5a}H^{5b}), 3.32 (1H, d, *J* 18 Hz, C*H*^{5a}H^{5b}), 1.64 (3H, s, CH_3); ^{13}C NMR (75 MHz, DMSO) δ_C 160.8, 156.4, 134, 130.7, 130.4, 126.7, 126.1, 125.9, 117.5, 115.5, 115.4, 115.2, 99.4, 69.2, 55.2, 43.9 (CH_2), 29.6 (CH_3); HRMS (ESI) calculated for $C_{22}H_{18}N_7O_2$: 412.1521 $(M+H)^+$, Found: 412.1500.

5.3 Determination of AChE and BChE inhibitory activity

Inhibitory activities of AChE and BChE were evaluated by using the Ellman's method.[34] Herein compounds **2(a-h)** and **5(a-h)** were evaluated as inhibitors of AChE and BChE. For initial screening each compound was dissolved in DMSO (end concentration of DMSO was less than 1% in assay) and tested at a final concentration of 0.5 mM. The compounds with considerable inhibition (more than 50%) were subjected to further analysis by making their 8 to 10 serial dilutions in assay buffer (50 mM Tris-HCl, 0.1 M NaCl and 0.02 M $MgCl_2$, pH 8.0). Reaction mixture comprised of 20 μL assay buffer, 10 μL of test compound, 10 μL of 0.031 U/mL of enzyme (0.5 and 3.4 U/mg of AChE or BuChE respectively). This mixture was incubated at 25 $^{\circ}$C for 10 min. After this pre-incubation, enzymatic reaction was started by addition of 10 μL of 1 mM acetylethiocholine iodide or butyrylthiocholine chloride (depending on the enzyme) and the mixture was incubated again for 15 min. The amount of enzymatic product was estimated by measuring change in absorbance at 405 nm using a microplate reader (Bio-Tek ELx 800TM, Instruments, Inc. USA). Neostigmine and donepezil were used as standard inhibitors. Enzyme dilution buffer consisted of 50 μM Tris HCl buffer containing 0.1% (w/v) bovine serum albumin (BSA) and pH 8. The effect of DMSO on activity of enzyme was subtracted by a negative control containing DMSO, instead of inhibitor. The IC_{50} values were calculated using non-linear curve fitting program PRISM 5.0 (GraphPad, San Diego, California, USA).

Conflict of interest

The authors have declared no conflict of interest.

Supplementary Information

The supplementary information includes the NMR spectra of tetrazole-1,2,5,6-Tetrahydronicotinonitriles **2(a-h)**.

Acknowledgement

We are thankful to Higher Education Commission (HEC), Pakistan and H. E. J. Research Institute of Chemistry, International Center for Chemical and Biological Sciences, University of Karachi, Karachi-75270, Pakistan for providing financial support of this project. Prof. Dr. Jamshed Iqbal is thankful to the Organization for the Prohibition of Chemical Weapons (OPCW), The Hague, The Netherlands and Higher Education Commission of Pakistan for the financial support through Project No. 20-3733/NRPU/R&D/ 14/520 for the financial support. Dr. Mariya al-Rashida is grateful to Dr. M. Saeed Iqbal and Rashid Masih for helpful discussions regarding thermal analysis.

6. References

[1] J. P. Hallett and T. Welton, Chem. Rev. 111 (2011) 3508-3576.

[2] J. H. Clark, Chem. Rev. 80 (1980) 429-452.

[3] A. R. Gangloff, J. Litvak, E. J. Shelton, D. Sperandio, V. R. Wang and K. D. Rice, Tetrahedron Lett. 42 (2001) 1441-1443.

[4] G. V. M. Sharma, V. G. Reddy, A. S. Chander and K. R. Reddy, Tetrahedron: Asymmetry 13 (2002) 21-24.

[5] C. Mukhopadhyay, P. Das and R. J. Butcher, Org. Lett. 13 (2011) 4664-4667.

[6] H. Karlsen, P. H. Songe, L. K. Sunsby, L. C. Hagen, P. Kolsaker and C. Romming, J. Chem. Soc., Perkin Trans. 1 (2001) 497-507.

[7] O. Di Pietro, E. Viayna, E. Vicente-García, M. Bartolini, R. Ramón, J. Juárez-Jiménez, M. V. Clos, B. Pérez, V. Andrisano, F. J. Luque, R. Lavilla and D. Muñoz-Torrero, Eur. J. Med. Chem. 73 (2014) 141-152.

[8] Desmond J. Brown, Jonathan A. Ellman and E. C. Taylor, The Chemistry of Heterocyclic Compounds, The Naphthyridines, John Wiley and Sons, Inc.Hoboken, New Jersey, 2008.

[9] D. Silva, M. Chioua, A. Samadi, P. Agostinho, P. Garção, R. Lajarín-Cuesta, C. de los Ríos, I. Iriepa, I. Moraleda, L. Gonzalez-Lafuente, E. Mendes, C. Pérez, M. I. Rodríguez-

Franco, J. Marco-Contelles and M. Carmo Carreiras, ACS Chem. Neurosci. 4 (2013) 547-565.

[10] P. Davies and A. J. F. Maloney, Lancet 308 (1976) 1403.

[11] P. J. Whitehouse, D. L. Price, A. W. Clark, J. T. Coyle and M. R. DeLong, Ann. Neurol. 10 (1981) 122-126.

[12] N. L. Batsch and M. S. Mittleman, World Alzheimer's Report 2012, 2012.

[13] K. Maslow, Alzheimers Dement. 6 (2010) 158−194.

[14] F. H. Darras, S. Pockes, G. Huang, S. Wehle, A. Strasser, H.-J. Wittmann, M. Nimczick, C. A. Sotriffer and M. Decker, ACS Chem. Neurosci. 5 (2014) 225-242 and reference therein.

[15] A. Castro and A. Martinez, Curr. Pharm. Des. 12 (2006) 4377-4387.

[16] D. Pratico, Ann. N.Y. Acad. Sci. 1147 (2008) 70-78.

[17] C. X. Gong and K. Iqbal, Curr. Med. Chem. 15 (2008) 2321-2328.

[18] A. Hameed, A. Anwar, S. Yousaf, K. M. Khan and F. Z. Basha, Eur. J. Chem. 3 (2012) 179-185.

[19] H. Karlsen, P. H. Songe, L. K. Sunsby, L. C. Hagen, P. Kolsaker and C. Rømming, J. Chem. Soc., Perkin Trans. 1 (2001) 497-507.

[20] Y. T. Abramenko, A. Ivashchenko, K. Nogaeva and Y. A. Sharanin, Chem. Heterocycl. Compd. 22 (1986) 508-512.

[21] Y. T. Abramenko, A. V. Ivashchenko, K. A. Nogaeva, N. A. Andronova and E. B. Putsykina, Zh. Org. Khim. 22 (1986) 264-269.

[22] Y. U. Abramenko, A. V. Ivaschchenko, K. A. Nogaeva, N. A. Andronova and E. B. Putsykina, J. Org. Chem. USSR (Engl. Transl.) 22 (1986) 230.

[23] F. M. Abdelrazek, N. H. Metwally, N. A. Kassab, N. A. Sobhy, P. Metz and A. Jaeger, J. Heterocyclic Chem. 47 (2010) 384-388.

[24] S. Dunkel, U. Heβ and G. Reck, J. prakt. Chem. 339 (1997) 414-419.

[25] M. J. Frisch, G. W. Trucks, H. B. Schlegel, G. E. Scuseria, M. A. Robb, J. R. Cheeseman, G. Scalmani, V. Barone, B. Mennucci, G. A. Petersson, H. Nakatsuji, M. Caricato, X. Li, H. P. Hratchian, A. F. Izmaylov, J. Bloino, G. Zheng, J. L. Sonnenberg, M. Hada, M. Ehara, K. Toyota, R. Fukuda, J. Hasegawa, M. Ishida, T. Nakajima, Y. Honda, O. Kitao, H. Nakai, T. Vreven, J. A. Montgomery Jr., J. E. Peralta, F. Ogliaro, M. J. Bearpark, J.

Heyd, E. N. Brothers, K. N. Kudin, V. N. Staroverov, R. Kobayashi, J. Normand, K. Raghavachari, A. P. Rendell, J. C. Burant, S. S. Iyengar, J. Tomasi, M. Cossi, N. Rega, N. J. Millam, M. Klene, J. E. Knox, J. B. Cross, V. Bakken, C. Adamo, J. Jaramillo, R. Gomperts, R. E. Stratmann, O. Yazyev, A. J. Austin, R. Cammi, C. Pomelli, J. W. Ochterski, R. L. Martin, K. Morokuma, V. G. Zakrzewski, G. A. Voth, P. Salvador, J. J. Dannenberg, S. Dapprich, A. D. Daniels, Ö. Farkas, J. B. Foresman, J. V. Ortiz, J. Cioslowski and D. J. Fox, Gaussian 09, 2009.

[26] P. C. Hariharan and J. A. Pople, Theor. Chim. Acta. 28 (1973) 213-222.

[27] A. D. Becke, J. Chem. Phys. 98 (1993) 5648-5652.

[28] C. Lee, W. Yang and R. Parr, J. Phys. Chem. 37 (1998) 785–789.

[29] T. Q. Hung, D. H. Hoang, N. N. Thang, T. T. Dang, K. Ayub, A. Villinger, A. Friedrich, S. Lochbrunner, G.-U. Flechsig and P. Langer, Org. Biomol. Chem. 12 (2014) 6151-6166.

[30] I. Javed, A. Khurshid, M. N. Arshad and Y. Wang, New J. Chem. 38 (2014) 752-761.

[31] H. Ullah, A.-u.-H. A. Shah, K. Ayub and S. Bilal, J. Phys. Chem. C. 117 (2013) 4069-4078.

[32] H. Ullah, A. Rauf, Z. Ullah, S. Fazl i, M. Anwar, A.-u.-H. A. Shah, G. Uddin and K. Ayub, Acta. A. Mol. Biomol. Spectrosc. 118 (2014) 210-214.

[33] M. A. Hashmi, A. Khan, K. Ayub and U. Farooq, Acta. A. Mol. Biomol. Spectrosc. 128 (2014) 225-230.

[34] G. L. Ellman, K. D. Courtney, V. Andres jr and R. M. Featherstone, Biochem. Pharmacol. 7 (1961) 88-95.

Graphical Abstract

One-Pot Synthesis of Tetrazole-1,2,5,6-Tetrahydronicotinonitriles and Cholinesterase Inhibition: Probing the Plausible Reaction Mechanism *via* Computational Studies

Leave this area blank for abstract info.

Abdul Hameed, Syeda Tazeen Zehra, Saba Abbas, Riffat Un Nisa, Tariq Mahmood, Khurshid Ayub, Mariya al-Rashida, Norbert Furtmann, Jürgen Bajorath, Khalid M. Khan, and Jamshed Iqbal

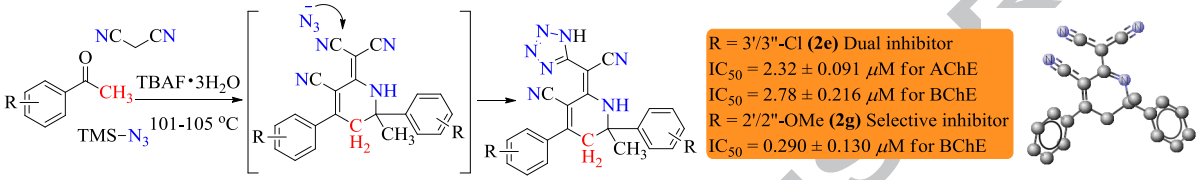

Research highlights

- A series of tetrazole-1,2,5,6-tetrahydronicotinonitriles was synthesized.
- Tetrazole-1,2,5,6-tetrahydronicotinonitriles as cholinesterase inhibitors.
- Plausible reaction mechanism was studied *via* computational methods.